Short communication

Influence of polymer additive on the performance of lead-acid battery negative plates

G. Petkova *, P. Nikolov, D. Pavlov

Institute of Electrochemistry and Energy Systems (CLEPS), Bulgarian Academy of Sciences, 1113 Sofia, Bulgaria

Available online 20 December 2005

Abstract

The effect of polyaspartate (PASP) on the performance of the lead-acid negative plate has been investigated. It was established that this polymer additive controls the crystallization process of lead sulphate and modifies the shape and size of $PbSO_4$ crystals. The addition of PASP to the negative paste and to the electrolyte improves the utilization of the negative active material and reduces the internal resistance of the negative plates.

The results obtained during cycling of lead-acid cells under simple simulated HRPSoC cycling duty with $2C$ discharge current show that addition of PASP improves the cycling ability of the negative plates and thus decreases the frequency of equalization charging during operation. A beneficial effect on the performance of lead-acid batteries was observed during HRPSoC cycling of flooded batteries with 0.1% PASP in the electrolyte. The addition of PASP leads to formation of smaller $PbSO_4$ crystals, which are more easily reduced during charge and hence prevents the accumulation of large lead sulphate crystals on the negative plates in HRPSoC duty.
© 2005 Elsevier B.V. All rights reserved.

Keywords: Lead-acid batteries; Negative plate; Polyaspartate; Crystal modifier; High-rate partial-state-of-charge duty

1. Introduction

Recently, the attention of the lead-acid battery industry has been focused on the application of VRLA batteries in the new-generation vehicles, particularly hybrid electric vehicles (HEV) and 42-V PowerNet automotive systems. These two applications require the battery to operate continuously at partial-state-of-charge (PSoC) and in addition to be charged and discharged at extremely high rates [1–3]. Investigations under simulated high-rate partial-state-of-charge (HRPSoC) duty have shown that the early battery failure is a result of accumulation of lead sulphate on the surface of the negative plates [4]. To overcome this process, dual-tab grid design [5,6] and trace element control [7] have been proposed. More recently, the use of expanded graphite [8,9] as additive that improves the conductivity during HRPSoC operation was demonstrated.

The accumulation of lead sulphate on the negative plates at HRPSoC regime indicates an ineffective charge reaction during this mode of operation. It is known that charging of the negative plate after deep discharge at a high rate is difficult [4,10].

In partial-state-of-charge operation, on the other hand, a certain amount of initially formed lead sulphate crystals remain throughout the cycling, as the cell is not fully charged. The presence of these $PbSO_4$ crystals provides conditions for recrystallization processes and formation of large $PbSO_4$ crystals [11]. Furthermore, discharge with high current generates high suppersaturation of Pb^{2+} and supports growth of smaller crystals, which also facilitate the recrystallization processes and growth of large $PbSO_4$ crystals. According to Ostwald–Freundlich equation, which gives the dependence of solubility on particle radius and surface free energy, larger crystals have reduced solubility. Thus, the dissolution of $PbSO_4$ (first step of the charge reaction at the negative plate) is impeded, the efficiency of charging decreases and the accumulation of lead sulphate on the negative plates increases. Therefore, if the process of recrystallization is limited, the negative plate failure during HRPSoC cycling will be delayed.

In this study we explored the above strategy to suppress the accumulation of lead sulphate on the negative plates under PSoC duty. Sodium salt of polyaspartic acid (PASP) has been selected from the commercially available functional polymers acting as crystal modifiers. Polyaspartates are water soluble dispersants having effect on the crystal morphology [12]. They are known to inhibit the precipitation of calcium carbonate, calcium sul-
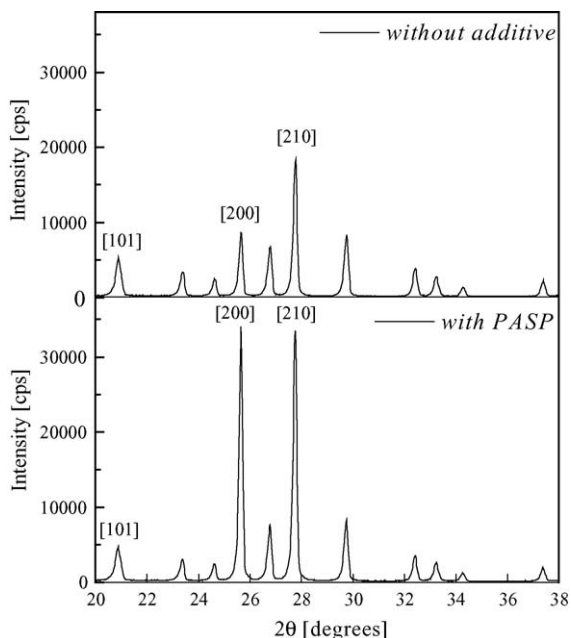
Fig. 1. XRD patterns for precipitated PbSO$_4$ obtained from Pb(NO$_3$)$_2$ and H$_2$SO$_4$ without and with 0.1% PASP.

phate and barium sulphate [13] and find an application as scale inhibitors and complexing agent for heavy metals [14–17].

The aim of the present work is to investigate the effect of PASP polymer additive on the recrystallization processes of lead sulphate in sulphuric acid solution. The polymer was introduced in the paste for negative plate and in the cell electrolyte. The effect of PASP on the performance of the negative plate subjected to simulated HRPSoC duty was also investigated.

2. Experimental

The effect of sodium salt of polyaspartic acid (Donlar Corp.) was tested as additive to the electrolyte and to the negative paste. For comparison, a reference cell (R-cell) without additive was tested, too. The cells with PASP in the electrolyte are denoted as PASP-E cells and these with PASP in the negative plate—as PASP-P cells. Three concentrations: 0.05, 0.1 and 0.2% PASP versus the weight of leady oxide, were applied during paste mixing. The concentrations of PASP in the electrolyte were 0.05, 0.1 and 0.2%.

Laboratory small-size lead-acid cells ($C_n = 0.1$ Ah) consisting of one negative and two positive electrodes were used for the tests. The negative pastes were produced using H$_2$SO$_4$ and leady oxide (LO) in a ratio equal to 6.0% (LO, 85% degree of oxidation). The expander formulation was: 0.2% Vanisperse A, 0.2% carbon black and 0.8% BaSO$_4$. The paste was applied to the small-size PbCa grid and was subjected to standard curing and drying, and multistep galvanostatic formation. All experiments with model cells were carried out in 1.28 s.g. H$_2$SO$_4$ at a temperature of 25 °C. The reference electrode was a Hg/Hg$_2$SO$_4$/H$_2$SO$_4$ (s.g. 1.28). The tests were performed using Arbin BT2043 potentiostat/galvanostat.

The phase composition of the negative active material was determined by X-ray diffraction analysis using ARD-15 PHILIPS diffractometer with Cu Kα radiation. Scanning electron microscopy (SEM) images were obtained on a JEOL 200 CX microscope. Chemical analyses were performed in order to characterize the negative active material after formation and at the different stages of cycling.

Flooded type SLI batteries 12/45 manufactured by Monbat Company (Bulgaria) were tested using Bitrode battery test modules.

3. Results and discussion

3.1. Effect of PASP on the crystal morphology of PbSO$_4$

Initially, the effect of PASP additive on the crystallization processes of PbSO$_4$ was established. For the purpose, lead sulphate was obtained by chemical precipitation [11] from saturated Pb(NO$_3$)$_2$ solution and 1.28 s.g. H$_2$SO$_4$ without and with addition of polymer additive. The deposit was filtered, washed and dried.

The XRD patterns for PbSO$_4$ obtained without additive and in the presence of 0.1% PASP are shown in Fig. 1. The preferential orientation of PbSO$_4$ crystals at [2 0 0] and [2 1 0] planes indicates the effect of PASP on the PbSO$_4$ crystallization. The SEM images of both types of lead sulphate crystals are presented in Fig. 2. A difference in crystal shape of PbSO$_4$ obtained without and with addition of polymer is evident.

The effect of PASP on the process of PbSO$_4$ recrystallization was also studied. The scanning electron micrographs in Fig. 3 show the PbSO$_4$ morphology after 1-week exposure of

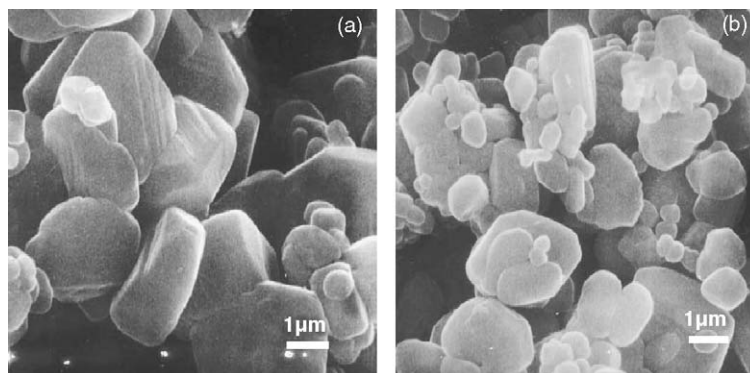Fig. 2. SEM micrographs of precipitated PbSO$_4$ obtained from Pb(NO$_3$)$_2$ and H$_2$SO$_4$: (a) without and (b) with 0.1% PASP.
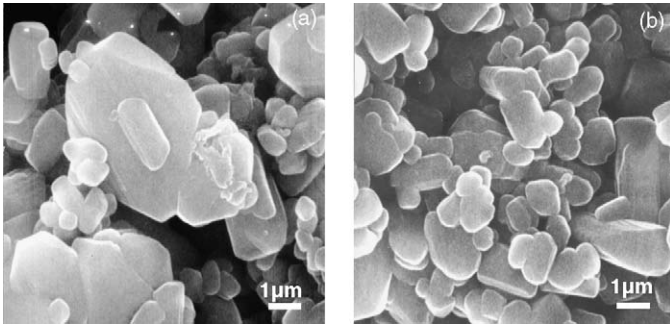
Fig. 3. SEM micrographs of precipitated PbSO$_4$ obtained from Pb(NO$_3$)$_2$ and H$_2$SO$_4$ after 1 week of recrystallization: (a) without and (b) with 0.1% PASP.

the obtained crystals to saturated PbSO$_4$ solution. It should be pointed out that the size of the PbSO$_4$ crystals obtained in the presence of polymer (Figs. 2b and 3b) remains almost unchanged after one week. This is an indication that the PASP additive slows down the recrystallization process of PbSO$_4$ and, probably, will prevent the formation of large PbSO$_4$ crystals during partial-state-of-charge operation.

3.2. Influence of PASP additive on the capacity of the negative plate

The effect of the polymer additive on the capacity of negative plate was tested at different rates (Peukert dependences). The negative electrode was discharged down to −0.6 V, which corresponds to 100% DOD. Tests with three levels of PASP in the paste and in the electrolyte were conducted. The results show that addition of 0.2 wt.% PASP to the electrolyte and 0.1 wt.% to the negative paste yields highest discharge capacity. Fig. 4 presents the discharge capacity obtained at different discharge rates for the reference cell and for the PASP-E cell with 0.2 wt.% PASP in the electrolyte and the PASP-P cell with 0.1 wt.% PASP in the paste. The additions of polyaspartate improve the utilization of the negative active material and thus enhance the cell capacity compared to the reference cell. The capacity of the cell with PASP added to the paste is higher than that of the cell with
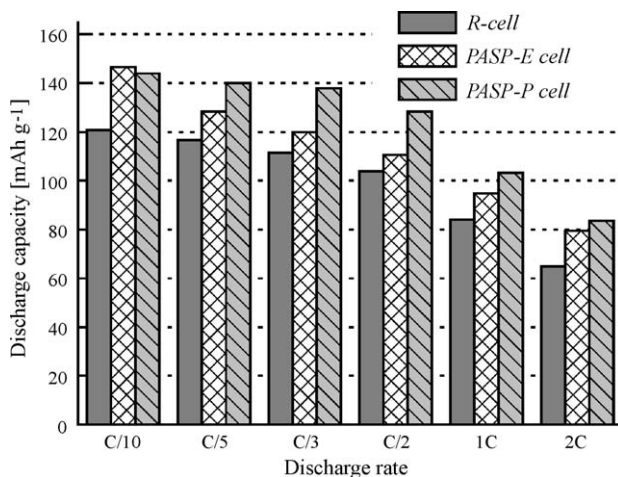

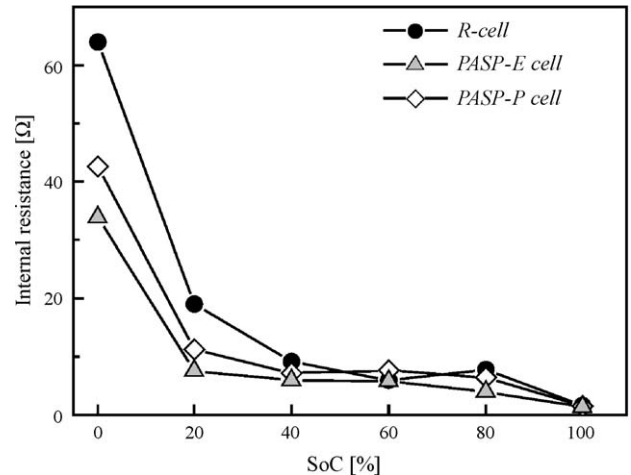Fig. 4. Discharge capacity of cells at different discharge rates.

Fig. 5. Dependence of internal resistance of tested negative plates on SoC.

PASP in the electrolyte. This difference is greatest on discharge with current C/3 and C/2 A.

Another important characteristic is the internal resistance of the negative plate. Fig. 5 illustrates the effect of PASP on the internal resistance of the negative plate (measured by employing pulse technique) at different state-of-charge (SoC). The addition of PASP to the electrolyte decreases substantially the resistance of the negative active material at lower state-of-charge. There is no difference between the internal resistances of the tested cells at SoC higher than 40%.

3.3. Performance of model cells under simulated HEV duty

The performance of model cells under simulated HEV duty conditions was tested by using simulated HRPSoC regime, described in Ref. [6]. The first step in this schedule was discharge at 1C rate to 50% SoC. After that, the cell was subjected to cycling according to the following scheme: charge at 2C rate for 1 min, rest for 10 s, discharge at 2C rate for 1 min, rest for 10 s. During this test the negative plate was cycled between 50 and 53% SoC. The negative plate potential was measured during cycling and the test was stopped when the potential reached −0.6 V. Fig. 6 illustrates the changes of the negative plate potential of a cell under simulated HRPSoC cycling.

The changes in end-of-discharge potential (EoDP) and end-of-charge potential (EoCP) during the above cycling mode were used to evaluate the effect of PASP on the negative plate performance. The results are presented in Fig. 7. For the R-cell, the end-of-discharge potential of the negative plate decreases slowly after 1300 cycles, while the end-of-charge potential increases to the region of hydrogen evolution after 1000 cycles. When subjected to the simulated HRPSoC cycling, cells with 0.1 wt.% PASP in the negative paste delivered 2700 cycles before the EoDP declined to −0.6 V and equalization charging was required. Similar result (2600 cycles) was obtained for the cells with PASP in the electrolyte. For comparison, the reference cell delivered 1900 cycles.

At the end of HRPSoC test, when the negative plate potential reached the cut-off-potential of −0.6 V, detailed analysis
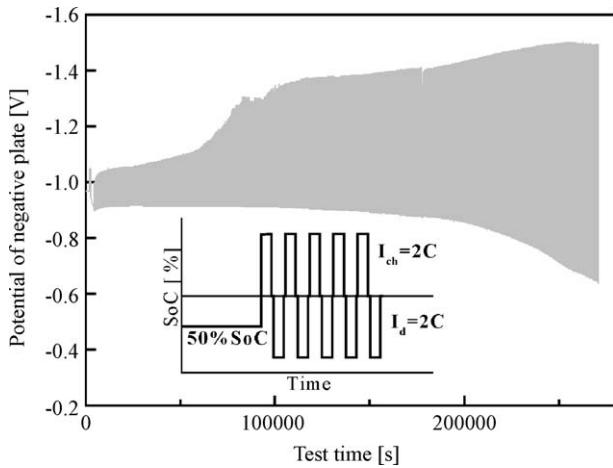
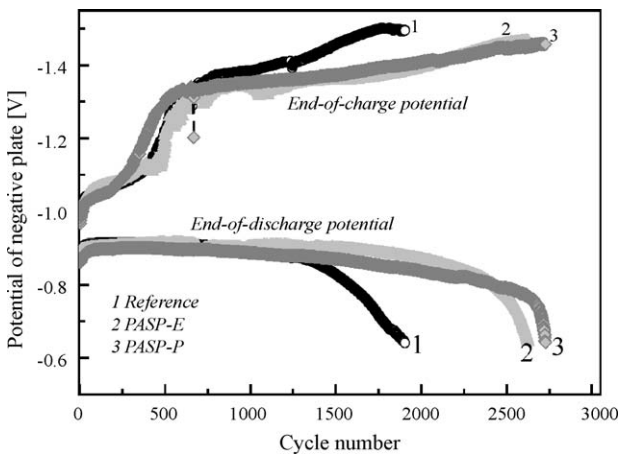Fig. 6. Changes in negative plate potential of R-cell under simulated HRPSoC cycling.

Fig. 7. End-of-charge and end-of-discharge potentials of tested negative plates during simulated HRPSoC cycling at 50% SoC.

Table 1
Results from chemical analysis of the negative active material at the end of HRPSoC test

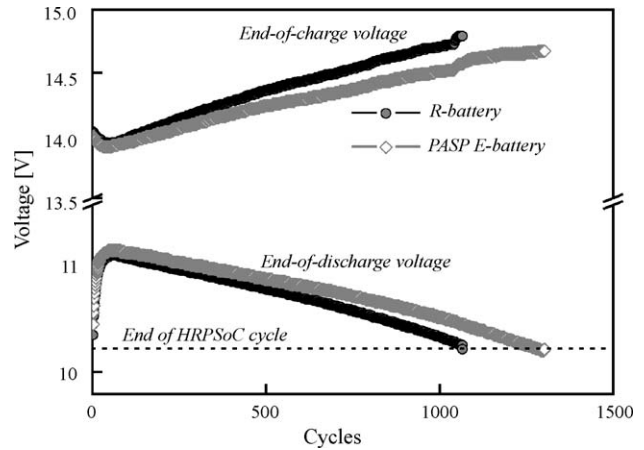| Type of cell	Cycles	PbSO$_4$ (%)
R-cell	1906	52.1
PASP-E cell	2627	54.0
PASP-P cell	2726	54.0

Fig. 9. End-of-charge and end-of-discharge voltage of batteries during cycling under simulated HRPSoC duty at 50% SoC.

The effect of PASP on the morphology of PbSO$_4$ crystals was established with SEM at the end of HRPSoC tests. Large polyhedral crystals of PbSO$_4$ can be observed on the surface of the negative plate from R-cell (Fig. 8a). The addition of PASP to the electrolyte (Fig. 8b) and to the negative paste (Fig. 8c) leads to formation of smaller PbSO$_4$ crystals. This is an indication that the introduction of crystal modifier preserves the small size PbSO$_4$ crystals in the negative active material during HRPSoC cycling and as a result delays the equalization charging of the battery.

3.4. Performance of batteries under simulated HEV duty

The effect of adding polymer additive to the electrolyte was tested on flooded type SLI batteries under simulated HRPSoC cycling. Fig. 9 presents the changes in the voltage of the reference battery and of the battery with PASP in the

of the negative active material was performed. A significantly high amount of lead sulphate was determined by chemical analysis (Table 1) indicating formation of "hard" sulphate during HRPSoC cycling. The values of PbSO$_4$ content obtained for the reference cell and for the cells with PASP were similar but it should be noticed that cells with additive endured about 30% longer cycling.
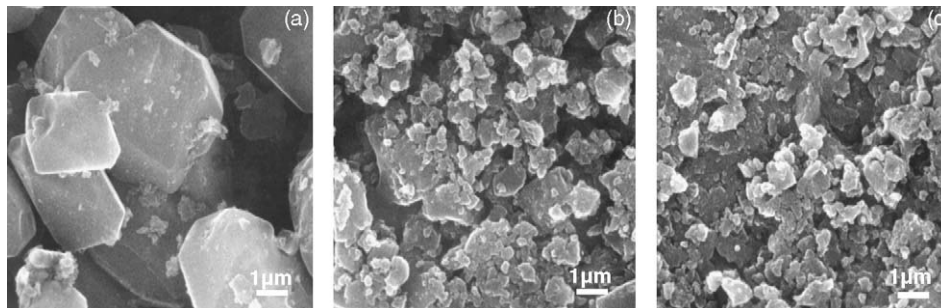

Fig. 8. SEM micrograph of the surface of the negative plate at the end of HRPSoC tests: (a) R-cell, (b) 0.2 wt.% PASP in the electrolyte and (c) 0.1 wt.% PASP in the negative paste.

electrolyte. The simulated HRPSoC test described above was applied to compare the effect of polymer additive on battery performance. The obtained results during cycling with $2C$ discharge/charge current show that addition of PASP to the electrolyte increases the number of partial charge–discharge cycles from 1060 for the R-battery to 1360 cycles for the battery with PASP in the electrolyte. Addition of polyaspartate affects noticeably the end-of-charge voltage, which is an evidence of improved charge efficiency.

4. Conclusions

The results of this investigation indicate that the use of polyaspartate as additive to the paste and to the electrolyte has a beneficial effect on the performance of the negative plate under HRPSoC operation. The additive controls the crystallization of $PbSO_4$ and modifies the shape and size of the crystals. The addition of PASP to the paste and to the electrolyte improves the utilization of the negative active material and reduces the internal resistance of the negative plate. The results obtained during cycling of lead-acid cells under simulated HRPSoC duty show that addition of PASP increases the cycling ability of the negative plates and thus decreases the frequency of equalization charging during operation. Initial performance data obtained from batteries with PASP in the electrolyte under HRPSoC cycling have shown promising results. Further tests of batteries are underway to verify the effect PASP on the electrical characteristics of the lead-acid battery and to elucidate the effect of chemical characteristics of polyaspartates on the processes of $PbSO_4$ formation and recrystallization.

References

[1] P. Moseley, D. Rand, J. Power Sources 127 (2004) 27.
[2] P. Moseley, J. Power Sources 133 (2004) 104.
[3] Cooper, L. Lam, P. Moseley, D. Rand, in: D.A.J. Rand, P.T. Moseley, J. Garche, C.D. Parker (Eds.), Valve Regulated Lead-acid Batteries, Elsevier, Amsterdam, 2004, p. 550.
[4] L.T. Lam, N. Haigh, C.G. Phyland, A. Urban, J. Power Sources 133 (2004) 126.
[5] M.J. Kellaway, P. Jennings, D. Stone, E. Crowe, A. Cooper, J. Power Sources 116 (2003) 110.
[6] L.T. Lam, R. Newnham, H. Ozgun, F. Fleming, J. Power Sources 88 (2000) 92.
[7] L.T. Lam, H. Ceylan, N. Haigh, J. Manders, J. Power Sources 107 (2002) 155.
[8] M.L.A. Hollenkamp, W. Baldsing, S. Lau, O. Lim, R. Newnham, D.A.J. Rand, J. Rosalie, D. Vella, L. Vu, ALABC Project N1. 2, Proceedings of the Advanced Lead-Acid Battery Consortium, Research Triangle Park, NC, USA, Final Report (July 2000–June 2002), 2002.
[9] Soria, J.C. Hernandez, J. Valenciano, A. Sanchez, F. Trinidad, J. Power Sources 144 (2005) 403.
[10] G. Petkova, D. Pavlov, J. Power Sources 113 (2003) 355.
[11] D. Pavlov, I. Pashmakova, J. Appl. Electrochem. 17 (1987) 1075.
[12] E. Burke, Y. Guo, L. Colon, M. Rahima, A. Veis, G.H. Nancollas, Colloids Surf. B: Biointerfaces 17 (2000) 49.
[13] R. Ross, K. Low, J. Shannon, Mater. Perform. 36 (4) (1997) 53.
[14] G. Schmitt, A.O. Saleh, Mater. Perform. 39 (8) (2000) 62.
[15] W. Hater, B. Mayer, M. Schweinsberg, PowerPlant Chem. 2 (2000) 12.
[16] M. Freeman, W. Hann, Y. Paik, G. Swift, Patent No. 5,531,934, 7 February 1996.
[17] J. Tang, S. Fu, D. Emmons, Patent No. 6,022,401, 2 August 2000.